

**INTELLIGENT DETECTION OF LARGE SCALE VOLCANISM DURING A SPACECRAFT FLYBY: EXAMPLES FROM FLYBYS OF IO.** M. K. Bunte<sup>1</sup>, Y. Lin<sup>1</sup>, S. Saripalli<sup>1</sup>, J. F. Bell III<sup>1</sup>, and R. Greeley<sup>1\*</sup>,  
<sup>1</sup>School of Earth and Space Exploration, Arizona State University, P.O. Box 871404, Tempe, AZ 85287  
 (Melissa.Bunte@asu.edu), \*in memoriam.

**Introduction:** The serendipitous discovery of eruptive events on Io [1] which indicate intense volcanic activity has led to a better understanding of Io's interior dynamics and encouraged the continued exploration of the outer solar system [2-4]. A desire to target events in future observations requires a characterization of the diverse physical nature of volcanic plumes and has prompted us to consider the range of conditions under which such features can be detected given mission constraints. Techniques for onboard data analysis enabling opportunistic observations have been introduced [5] and shown to be scientifically valuable [6].

Here, we illustrate the effectiveness of autonomously detecting eruptive events using images taken during flybys of Io. The distinct appearance of plumes [7, 8] allows for ideal detection when visible on the limb. Plumes populate a large portion of the satellite and many are visible against the background surface rather than on the limb. Telltale characteristics indicate their difference from the highly varied background surface [7]. We positively identified 73-95% of known volcanic plumes on Io in each of the three flyby datasets. We outline the conditions for detecting large scale features like those viewed at Io and discuss the importance of establishing detection techniques to enable detection of smaller features at other bodies in the context of future flyby observations at those targets.

**Method:** We applied a Scale Invariant Feature Transform (SIFT) [9] to selected single and sequential single-band images of Io taken with *Voyager's* narrow- and wide-angle cameras, *Galileo's* SSI, and *New Horizons's* LORRI where plumes have been manually detected. SIFT produces interest points and associated descriptors based on the magnitude and orientation of brightness gradients near each point (Figure 1, left). Descriptors are invariant to illumination or viewpoint changes, noise, rotation, and scaling. We use these characteristics to minimize the number of images needed to establish a database of activity type examples. In a selected set of images, each descriptor is manually categorized according to the presence or absence of a plume. Descriptors that positively identify a feature constitute a database for comparison with images of unknown content; we generated a unique database for each mission dataset. By means of a supervised classifier such as *k*-Nearest Neighbor (*k*NN) [10], unreviewed images may be processed with SIFT and compared to the database of descriptors to autonomously

identify plumes. The classifier determines the value of each interest point by comparing points within a specified Euclidean distance (Figure 1, right).

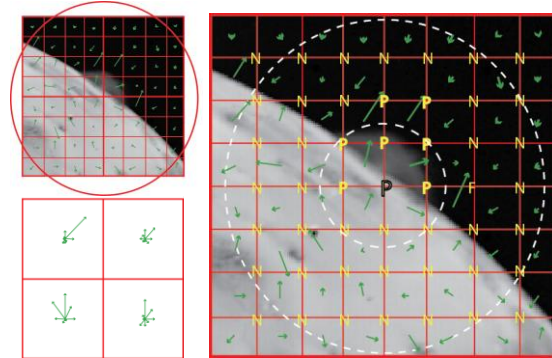


Fig. 1. SIFT descriptors [as in 9]: The gradient magnitude and orientation (arrows, UL) at each sample near the point of interest are binned by subregion (here, a 4x4 grid; LL) to generate histograms. *k*NN Classification [R, as in 10]: For threshold distance  $k=1$  (inner circle); the sample is classified as positive. For  $k=3$  (outer circle), the sample is classified as negative. Point F at center right is a potential misclassification; it shows a gradient similar to the manually defined positive feature. [*Galileo* base image, NASA/JPL.]

**Results:** Sequential images offer similar views and can increase detection rates. The selection of images used to test this approach is not limited by the amount of the planetary disk or limb that is visible or by the placement of strong edges that appear in the scene. The greatest limitations on image appearance are the phase angle and degree of overexposure; a distinct albedo gradient is necessary to produce interest points. Of the 20 volcanic centers on Io known to produce explosive volcanic columns [7, 11], we have successfully detected at least 12 of the plume dust columns (Table 1).

Plume	Detection	Location	Plume	Detection	Location
Acala	Possible	in eclipse	Maui	Y	
Amirani	Y	limb	Pele	Possible	
Culann	Y	limb	Pillan	Y	limb
Kanehekili	N		Prometheus	Y	limb
Kurdalagon	Possible		Ra	Y	limb
Lerna	Y	limb	Thor	Y	limb
Loki	Possible	terminator	Tvashtar	Y	limb
Marduk	Y	faint	Volund	Possible	
Masubi N	Y	terminator	Zal	Possible	terminator
Masubi S	N	unresolved	Zamama	Y	limb

Table 1. Detection of known plumes. Sources where deposits are seen but plume dust/gas columns have not been identified (e.g. Surt, Aten) are not included.

SIFT descriptors mainly result from surface material gradients and background noise, yielding a high ratio of negative to positive features in database training. However, SIFT+kNN detected plumes of different shapes, sizes, and orientations as well as in locations other than the limb (Figure 2). Detections were successful regardless of noise and image artifacts but failed with misclassification and in overexposure. In all cases, false negatives occurred when plumes were less than 9 pixels in size regardless of position or orientation. This size restriction is controlled by viewing conditions rather than by the vertical height of the plume.

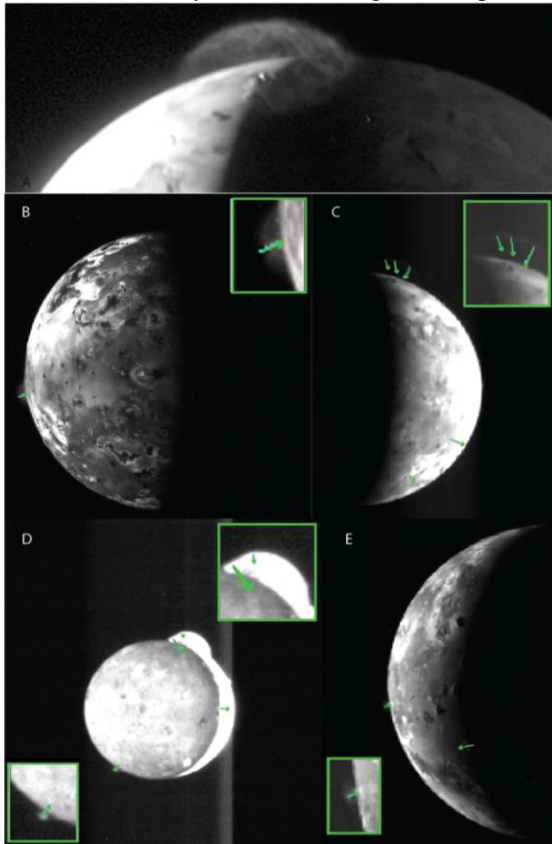


Fig. 2. A [*New Horizons*]. Tvashtar plume viewed at the terminator. B [*Galileo*]. Positive detection of the Pillan plume in limb view; Prometheus plume and shadow not detected. C [*New Horizons*]. Tvashtar plume detected on the limb, multiple keypoints are necessary for large objects; false positives near the limb result from non-uniform brightness due to overexposure. D [*New Horizons*]. Positive detections of the Tvashtar (top) and Lerna (bottom) plumes; the Masubi plume at the terminator does not have a sufficient gradient compared to the overexposed limb. E [*Galileo*]. Positive detection of the Culann plume; an additional feature is detected at the terminator.

The highest detection rates are for *Voyager* images, at 92-95%. We attribute this to resolution differences dictated by both the imaging optics and flyby distance which in turn limits the variety of plume columns that are detectable. In *Galileo* and *New Horizons* images, increased resolution and brightness contrasts imposed by exposure differences increase the variety of plume

characteristics visible and limit the margin of detection based on brightness gradient, respectively. Resulting classification rates using a small descriptor database are significantly lower at 67-74%.

**Discussion: Ideal databases.** Building a database which represents the full range of observed, expected, and unknown feature characteristics is essential to yield the most effective data from future missions, where mission lifetime and data-limiting conditions will preclude real- or near real-time human interaction for identifying sites of geophysical activity on the planetary targets to be observed. However, the unknown nature of potential features will require a flexible database to avoid missed detection of valuable data.

**Increasing detection.** Altering the selection of images used to build the comparison database, increasing the database size, and varying or combining multiple methods of classification [6] produce a range of results. Classification with kNN yields the highest detection rate of any single classification technique, though combining techniques for repeated comparison can increase detection rate at the expense of increased false detection. This implies that combining multiple autonomous techniques where processing constraints allow can increase science return. If the qualities of a plume or other feature are known and remain consistent relative to parent planet or resolution, we find that a minimal database can be established even with increased positive detections [12]. Additionally, we find that onboard image calibration can, in certain instances, increase the ability to identify and classify plumes correctly, particularly when they are not faint [12].

**Future Work:** Future work includes the application of this method to the remainder of all planetary images where plumes or jets are known or suspected to exist to establish criteria for detecting unknown events at targets with suspected geophysical activity. The Prometheus plume seen in nadir view in Fig. 2B is not detected, nor is its shadow, suggesting that an additional feature class based on the characteristics of a plume deposit is needed to successfully detect all active volcanic plumes. An effort to establish a database for distinguishing plume deposits from the vertical columns will allow examination of surface and nadir views to reveal evidence of activity that may not be powerful enough to produce explosive events.

**References:** [1] Morabito, L.A. et al. (1979) *Science* 204, 972. [2] Smith, B. et al. (1979) *Science* 206, 927. [3] Porco, C. et al (2006) *Science* 311, 1393. [4] A'Hearn, M.F. et al. (2011) *Space Sci.* 332, 1396. [5] Thompson, D.R. et al. (2011) *Planet. & Space Sci.* doi:10.1016/j.pss.2011.11.006. [6] Lin, Y. et al. (2012) *IEEE ICRA*, 3431. [7] Geissler, P.E. and Goldstein, D.B. (2007). In: *Io After Galileo*, Lopes, R.M.C. and Spencer, J.R. (Eds.), 162-192. [8] Lopes-Gautier, R. et al. (1999) *Icarus* 140, 243. [9] Lowe, D.G. (2004) *Int'l Jour. Computer Vision* 60, (2), 91. [10] Cover, T.M. and Hart, P.E. (1966) *Trans. Info. Theory*, 13 (1), 21. [11] Spencer, J. et al. (2007) *Science* 318, 240. [12] Lin, Y. et al. (submitted) *JFR*.